Charge-state dependence of *K*-shell x-ray production in aluminum by 2–12-MeV carbon ions

H. L. Sun, Y. C. Yu, E. K. Lin, and C. W. Wang
Institute of Physics, Academia Sinica, Nankang, Taipei, Taiwan 11529, Republic of China

J. L. Duggan, A. R. Azordegan, and F. D. McDaniel
Ion Beam Modification and Analysis Laboratory, Department of Physics, University of North Texas, Denton, Texas 76203

G. Lapicki
Department of Physics, East Carolina University, Greenville, North Carolina 27858
(Received 7 November 1995)

Charge-state dependence for *K*-shell x-ray production cross sections in $_{13}$Al bombarded by 2–12-MeV $_{6}$C ions with charge states from 2+ to 6+ was measured using a Si(Li) detector. A thin Al target was used to ensure single collision conditions. Contributions of the electron capture as well as direct ionization to the inner-shell ionization were determined by an analysis of the charge-state dependence of the target x-ray production. The measurements are compared with the prediction of the ECPSSR theory using a single-hole fluorescence yield. The ECPSSR theory is based on the perturbed stationary state (PSS) formalism and relativistic effects (R) for the target electrons, and energy loss (E) and Coulomb deflection (C) of the projectile. In general, this theory gives reasonable agreement with the data for carbon ions without *K* vacancies while it overpredicts the data for carbon ions with *K* vacancies. The significant underprediction of the data at the lowest energy is likely associated with the molecular-orbital effect that is not accounted for in the ECPSSR theory. [S1050-2947(96)05706-X]

PACS number(s): 34.70.+e, 34.50.Fa

I. INTRODUCTION

Inner-shell ionization produced by charged particles has been studied intensively in recent decades. The literature for *K*-shell x-ray studies indicates a strong need for heavy-ion measurements to clarify the noticeable deviation of the theoretical calculations from the data. Electron capture (EC) to projectile vacancies has been shown to enhance target x-ray yields for heavy-ion impact [1]. It is known that direct ionization (DI) is nearly independent of the projectile charge state for inner electronic shells. Previous work by McDaniel *et al.* [2] for 52-MeV $_{14}Si^{q+}$ ions incident on $_{22}$Ti, $_{29}$Cu, and $_{32}$Ge discussed projectile electron–target-electron interaction as a possible mechanism that could enhance the target *K*-shell x-ray production with increasing number of electrons on the projectile. However, the present data for incident $_{6}C^{q+}$ ions with two or more electrons bombarding $_{13}$Al did not exhibit any differences in x-ray production cross sections. It also has been observed that if electron capture contributions are included, then theories give a better fit to the experimental results of these complex heavy-ion interactions. Inner-shell ionization in ion-atom collisions proceeds through three basic channels: DI [3], EC [4], and the molecular-orbital (MO) promotion [5]. These channels become important in various regions of the Madison and Merzbacher figure [6] that classifies collision systems according to two parameters: Z_1/Z_2 and v_1/v_{2S}, where Z_1 and Z_2 are the respective atomic number of the incident ion and the target atom, v_1 is the velocity of the ion, and v_{2S} is the velocity of the target inner *S*-shell ($S=K$, L, M, etc.) electron. DI of the target inner-shell electron to the continuum dominates the interaction for strongly asymmetric and fast collisions where $Z_1/Z_2 \ll 1$ and $v_1/v_{2S} \gg 1$. For the less symmetric collisions, EC or charge transfer to vacancies in the ion passing the target becomes important. This is valid for the region $Z_1/Z_2 \leqslant 1$ and $v_1/v_{2S} \leqslant 1$. The MO promotion comes into play in symmetric and very slow collisions where $Z_1/Z_2 \approx 1$ and $v_1/v_{2S} \ll 1$. First-order Born or equivalent approximations—such as the plane-wave Born approximation (PWBA) [3,7], the semiclassical approximation (SCA) [8], and the binary encounter approximation (BEA) [9]—give noticeable deviations when compared to the available experimental results of heavy-ion collisions. With the addition of a semiempirical EC to the existing DI theoretical cross sections for the inner-shell ionization, Gardner *et al.* [10] obtained good agreement between the theory and experiment for $_{29}$Cu *K*-shell x-ray production by incident ions from hydrogen to chlorine. The EC contribution was introduced by Nikolaev's [Oppenheimer-Brinkman-Kramers-Nikolaev (OBKN)] development [11] of the Oppenheimer-Brinkman-Kramers [12,13] theory. It was proposed [10] that the OBK calculations should be scaled down by semiempirical factors to fit the experiment. By going beyond the first-order Born approach, the ECPSSR theory (Brandt and Lapicki [14] for DI plus Lapicki and Losonsky [15] and Lapicki and McDaniel [16] for EC) achieved overall better agreement with the data [17,18]. The predictions of EC have been extensively investigated; however, as yet no comprehensive studies have been made in which charge-state effects were systematically considered. The ECPSSR theory is based on the perturbed stationary state (PSS) formalism and relativistic effects (R) for the target electrons and energy loss (E) and Coulomb deflection (C) of the projectile.

The contribution of EC as well as DI can be inferred from charge-state dependence of target x-ray prediction. The targets must be very thin so that the interaction occurs clearly in

TABLE I. *K*-shell x-ray production cross sections (in kilobarns) of aluminum by ${}_6C^{q+}$ ions with energies E_1 from 2 to 12 MeV, for charge state $q+$. σ_{KX} are the measured *K*-shell x-ray production cross sections for the 0.14-μg/cm^2 aluminum. $\sigma_{KX}^{\mathrm{ECPSSR}}$ are the *K*-shell x-ray production cross sections taken as a product of *K*-shell ionization cross section according to the ECPSSR theory and the *K*-shell x-ray fluorescence yield in ${}_{13}$Al according to Krause [49]. Ratios of the measured cross sections to the ECPSSR prediction, $\sigma_{KX}/\sigma_{KX}^{\mathrm{ECPSSR}}$ and v_1/v_{2K}, are shown in the last two columns, where v_1/v_{2K} is the projectile velocity scaled by the orbital velocity of the target *K*-shell electron.

E_1 (MeV)	$q(+)$	σ_{KX} (kb)	$\sigma_{KX}^{\mathrm{ECPSSR}}$ (kb)	$\sigma_{KX}/\sigma_{KX}^{\mathrm{ECPSSR}}$	v_1/v_{2K}
2	2	0.058±0.008	0.022	2.62	
2	3	0.056±0.008	0.022	2.51	0.20
2	4	0.058±0.010	0.023	2.60	
4	2	0.67±0.08	0.83	0.81	
4	3	0.64±0.09	0.83	0.77	0.29
4	4	0.67±0.09	0.83	0.80	
4	5	1.10±0.15	2.4	0.46	
6	2	3.6±0.5	4.5	0.79	
6	3	3.5±0.5	4.5	0.76	
6	4	3.6±0.5	4.6	0.78	0.35
6	5	5.2±0.7	10.7	0.48	
6	6	10.6±1.7	16.7	0.63	
8	3	9.2±1.6	11.4	0.81	
8	4	9.2±1.7	11.5	0.80	0.41
8	5	14.7±2.4	23.7	0.62	
8	6	23.1±3.9	33.9	0.68	
10	3	13.6±2.1	19.7	0.69	
10	4	15.7±2.3	19.9	0.79	0.46
10	5	21.1±3.3	37.6	0.56	
10	6	34.2±7.9	55.3	0.62	
12	4	15.4±3.2	28.3	0.54	
12	5	21.9±4.6	49.9	0.44	0.50
12	6	31.3±7.8	71.6	0.44	

the single collision realm [1,19,20]. For the present measurements, the experiment was performed with a 0.14-μg/cm^2 ultrapure aluminum target. The charge-state dependence data—which will be discussed in Sec. II—establish that this target is indeed thin enough so that single collisions dominate over multiple collisions in the ionization process. Accelerator studies of charge-state dependence were reported in 1972 by Macdonald *et al.* [1]. Their work was followed by additional papers from the same group [21] as well as from other pioneers in this field [22–24]. A theoretical paper [4] suggested that the Z_1 dependence of the x-ray yield could be accounted for by charge exchange into bound states of the fully stripped projectile. These early calculations stimulated additional measurements [10,20,25–34] at Kansas State University. We have been involved with such a charge-state dependence investigation of *K*-, *L*-, and *M*-shell ionization since 1977 [35–41].

In the present work, *K*-shell x-ray production in ${}_{13}$Al was measured for incident carbon ions with charge states between 2+ and 6+ and an energy range from 2 to 12 MeV. To ensure that the ultrapure ${}_{13}$Al target was thin enough to be in the single collision realm, a wide variety of measurements of the x-ray yields versus target thickness were made as a function of both energy and charge state. These data showed that the single collision regime was attained for targets with thickness less than 0.3 μg/cm^2. All of the measurements reported in Tables I and II are for a 0.14-μg/cm^2 ${}_{13}$Al target. The EC cross sections were deduced by subtracting the single collision data taken with carbon ions with filled *K* shells (i.e., $q=2-4$) from those obtained with the fully stripped and single-electron ${}_6$C ions. From a systematic comparison of the data, it is possible to obtain the *K*-shell x-ray production cross sections produced by both DI and EC. Our study covers the range $0.2 \leqslant v_1/v_{2K} \leqslant 0.5$ at $Z_1/Z_2=0.46$.

II. EXPERIMENTAL PROCEDURE

The experiment was performed using a 3-MV tandem accelerator at the University of North Texas. The experimental

TABLE II. Contribution of electron capture to K-shell x-ray production cross sections $\sigma_{KX}^{\mathrm{EC}}(q)$ (in kilobarns) in Al by carbon ions with K vacancies ($q=5$ and 6) at energies $E_1=4-12$ MeV. The experimental K-shell x-ray production cross sections due to electron capture, $\sigma_{KX}^{\mathrm{EC}}$ ($q=5$ or 6), were calculated from the difference of Al K-shell x-ray cross sections, i.e., $\sigma_{KX}(q=5$ or 6) $-\sigma_{KX}(q=4$ or 3), for carbon ions with and without K vacancies. The $\sigma_{KX}^{\mathrm{EC-ECPSSR}}$ is the Al K-shell x-ray production due to electron capture from the aluminum K shell according to the ECPSSR theory.

E_1 (MeV)	q (+)	$\sigma_{KX}^{\mathrm{EC}}(q)=\sigma_{KX}(q)-\sigma_{KX}(q=4)$ (kb)	$\sigma_{KX}^{\mathrm{EC-\ ECPSSR}}(q)$ (kb)	$\sigma_{KX}^{\mathrm{EC}}(q)/\sigma_{KX}^{\mathrm{EC-ECPSSR}}(q)$	v_1/v_{2K}
4	5	0.43±0.18	1.6	0.28	0.29
6	5	1.6±0.8	6.5	0.25	0.35
6	6	7.1±1.8	12.6	0.56	
8	5	5.5±2.9	13.5	0.41	0.41
8	6	13.9±4.3	24.9	0.56	
10	5	5.5±4.0	20.1	0.27	0.46
10	6	18.6±8.2	37.8	0.49	
12	5	6.5±5.6	24.3	0.26	0.50
12	6	16.0±8.5	46.8	0.34	
E_1 (MeV)	q (+)	$\sigma_{KX}^{\mathrm{EC}}(q)=\sigma_{KX}(q)-\sigma_{KX}(q=3)$ (kb)	$\sigma_{KX}^{\mathrm{EC-\ ECPSSR}}(q)$ (kb)	$\sigma_{KX}^{\mathrm{EC}}(q)/\sigma_{KX}^{\mathrm{EC-ECPSSR}}$	v/v_{2K}
4	5	0.46±0.17	1.6	0.30	0.29
6	5	1.7±0.8	6.5	0.26	0.35
6	6	7.2±1.7	12.6	0.57	
8	5	5.5±2.8	13.5	0.41	0.41
8	6	13.9±4.2	24.9	0.56	
10	5	7.6±3.9	20.1	0.38	0.46
10	6	20.7±8.2	37.8	0.55	

procedures, details, and setup have been described in previous papers [40,41]. The 3-MV tandem is not capable of producing large quantities of highly stripped $_6$C ions and therefore a post acceleration foil stripping chamber was added immediately after the tandem. It was found that the so-called ''super strong'' stripping foils [42] had sufficient lifetime to do the experiment. The basic difficulty is that these foil strippers have to withstand the total beam flux from the tandem for a long period. Some of the single data points required as much as 15 h of beam time to acquire reasonable statistics in the peaks of interest. When a foil breaks during a run, it is necessary to start over at that energy because the stripper foils vary slightly in thickness and hence the dE/dx may critically change the magnetic field setting necessary for the charge state being studied. The magnetically selected charge state of proper energy was directed onto the Al target through a pair of collimating slits that gave a 1-mm^2 beam spot. To overcome the current integration problem, which is always present for highly charged, heavy ions, the Rutherford scattered ions were simultaneously measured at 45° and 169°. In the cross-section determination, the simultaneous measurements of scattered ions and x rays eliminate the need for the measurement of both the number of incident ^{12}C ions and the number of target nuclei per cm^2. The efficiency of the x-ray detector has been the subject of several studies by our group [43], and by now this efficiency as a function of x-ray energy is very well known. The Al targets were produced by evaporating ultrapure aluminum onto 5-μg/cm^2 carbon foils that had been previously cleaned by techniques that were developed and described previously [37,44,45]. Measurements of these carbon foils show that contaminant elements on the cleaned targets have effective thicknesses of less than 1 ng/cm^2. The aluminum K-shell x-ray spectra were therefore very clean even with run times of 15 h.

As mentioned above, the single collision region was found by making a series of Al targets from 12.5 to 0.14 μg/cm^2. The ''effective'' K-shell x-ray production cross sections were measured as a function of the target thickness for each target at an energy of 8 MeV for charge states 3+, 4+, 5+, and 6+. Figure 1 shows that at 0.14 μg/cm^2 the single collision regime is clearly established. To calculate the ''effective'' x-ray production cross sections exhibited in Fig. 1, corrections for target thickness and x-ray attenuation were made. The following expression was used:

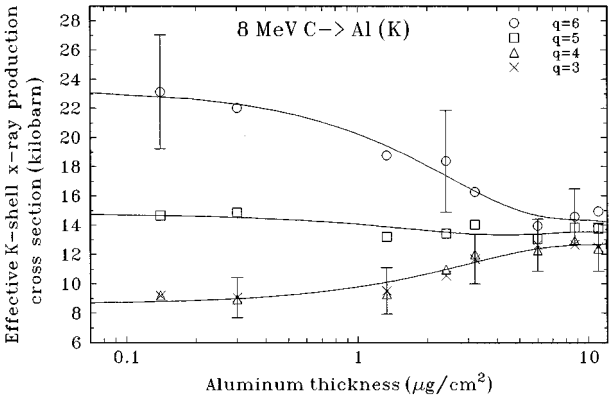

FIG. 1. ''Effective'' *K*-shell x-ray production cross sections in aluminum as a function of the thickness of the Al target for 8-MeV carbon ions with charge states 3+, 4+, 5+, and 6+. The curves are polynomial fits to these data.

$$\sigma_{KX}=\frac{(d\sigma_R/d\Omega)d\Omega\,\tau_X Y_{KX}}{Y_R\tau_R\epsilon}\left(1-\frac{\Delta E}{E_1}\right)^{-(s-2)}\left(\frac{\mu t}{1-e^{-\mu t}}\right), \tag{1}$$

where Y_{KX} is the yield under the *K* x-ray peak, ϵ the efficiency of the Si(Li) detector for the Al $K\alpha$ peak, $d\sigma_R/d\Omega$ the theoretical Rutherford differential scattering cross section (in barns per steradian), $d\Omega$ the particle detector's solid angle (in steradian), Y_R the Rutherford scattering yield, τ_X and τ_R the dead time corrections for x rays and scattered particles, respectively, ΔE the energy loss of the ion in the finite thickness of the target ($\Delta E=55$ keV as calculated using TRIM90 [46] for the thickest target used in the present work), *s* the exponent in the energy dependence of the x-ray production cross section [47] ($s=3.4$ for the present 8-MeV data), the power of -2 in the same exponent reflects the inverse square dependence of the Rutherford scattering cross section on the energy E_1 of the ion, μ is the mass absorption coefficient for the Al *K* x rays [48], and *t* the target thickness which was measured by a quartz crystal thickness monitor and confirmed by the Rutherford backscattering with 1.5-MeV α particles. The Al target (0.14 μg/cm^2) used for the charge-state dependence experiment was sufficiently thin to neglect the energy loss of the beam and x-ray attenuation within the target.

The uncertainties in this experiment are estimated to be between 12% and 25%, including errors from x-ray counting statistics 5–12 % after background stripping and curve fitting, Rutherford scattered particle counting statistics 4–18 % due to background, x-ray detector efficiency 12%, solid angles of the particle detector 1.3%, Rutherford differential cross section 2%, and beam energy 1.5%.

III. RESULTS AND DISCUSSION

From the ''effective'' cross-section measurements for various incident charge states shown in Fig. 1, it can be seen that for a thickness above 6 μg/cm^2 the ''effective'' cross section for all incident ions is nearly constant (at about 13.5 kb). Therefore, for targets thicker than 6 μg/cm^2, all incident ${}_6C^{3+,4+,5+,6+}$ ions reach the equilibrium charge state in the target. The plateau was found in the data trend for each charge state of the measured cross sections. It can been seen that the single collision region is reached at thicknesses less than about 0.3 μg/cm^2. As mentioned above, all DI and EC data reported in this paper are based on a 0.14-μg/cm^2 ${}_{13}$Al target (i.e., about 5 Å aluminum foil).

Table I gives a summary of the measured cross sections for Al *K*-shell x-ray production for the 0.14-μg/cm^2 target. Data are presented as the ratios of the experimental *K*-shell x-ray production cross section to the ionization cross sections of the ECPSSR theory multiplied by the single-hole fluorescence yield of Krause [49]. These ratios are displayed as a function of the projectile energy as well as its velocity scaled by the target *K*-shell electron velocity, v_1/v_{2K}.

Multiple ionization due to the bombardment of a target with heavy charged particles could possibly change the fluorescence yield for the *K* shell [50]. The single-hole fluorescence yield may be inadequate when a large amount of multiple ionization of the target atom is induced by heavy-ion impact. Multiple ionization perturbs the electron binding levels since it reduces the screening of the nuclear charge. Richard and co-workers [51–54] showed that the multiple inner-shell vacancies produced by heavy-ion–atom collisions lead to the measurable energy shift of the emitted x rays. The main question is, how do multiple vacancies affect the fluorescence yield in aluminum? There is no exhaustive set of data in the literature to provide definite answers [20,55,56]. Multiple ionization as well as the x-ray fluorescence yield vary with the type of primary ion and depend on its charge state and energy. Tawara *et al.* [32] showed that the *K*-shell fluorescence yield was fairly constant for a solid ${}_{14}$Si target but did show variation for SiH_4 gas targets for incident ${}_9F^{q+}$ ions. A host of other studies have been made [19,22,31,55,56] but the most convincing set of data for the current case was presented by Tunnel, Can, and Bhalla [57]. In their study, the energy dependence of the fluorescence yield in a solid Ti target for the incident ions ${}_1$H through ${}_{17}$Cl with projectile energies 0.5–4.5 MeV/u was analyzed. For ${}_6$C ions, ω_K varied from 0.225 to 0.243, which is merely an 8% variation.

Although ${}_6$C bombardment of ${}_{13}$Al is expected to create more multiple vacancies than in ${}_{22}$Ti of the Tunnell *et al.* experiment, the fluorescence yield may not rise as dramatically. The competition between the radiative and nonradiative vacancy decays is constrained in lighter elements that lack a full complement of electrons in their *L* and *M* shells. Using the formulas of Tanis *et al.*, [58] we find that even with the most favorable distribution of vacancies in Al to maximize the x-ray vis-à-vis Auger-electron transitions (which is obtained when there are four vacancies in the $2p$ state and none in the $3p$ state) the fluorescence yield is enhanced by 25%. The ${}_7$N on ${}_{13}$Al *K*-shell x-ray yield spectrum of Knudsen *et al.* [59] is consistent with almost five vacancies in the $2p$ state which, using the formulas of Tanis *et al.*, [58] would result in a 15% enhancement relative to the single-hole fluorescence yield. Therefore, in our ionization-to-x-ray production conversion we employ the single-hole fluorescence yield [49].

Figure 2 shows projectile charge-state dependence of the *K*-shell x-ray production cross sections of ${}_{13}$Al for 2–12-MeV carbon ions. It is noted that the cross sections for charge states 2+, 3+, and 4+ at 2–8 MeV are almost the

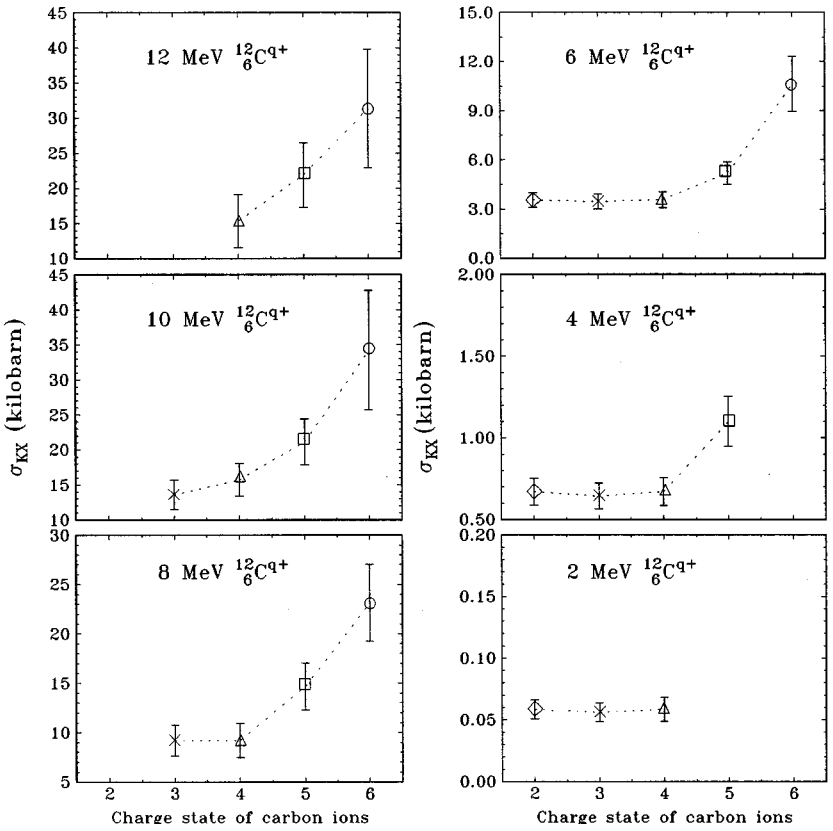

FIG. 2. Charge-state dependence of K-shell x-ray production cross sections in a 0.14-μg/cm^2 $_{13}$Al target for 2–12-MeV carbon ions with charge state from 2+ to 6+.

same, indicating that the electron capture contribution for carbon ions without a K vacancy (EC to L, M, ... shells of the carbon ion) is small compared to that for carbon ions with K vacancies for charge states 5+ and 6+ (EC to K, L, M, ... shells of carbon ions). At 10 MeV, the cross section for charge state 4+ is slightly higher than that for charge state 3+. This is attributed to the formation of the $1s2s$ metastable state when heliumlike carbon ions pass through the postaccelerator stripper [60,61] and the fact that a fraction of metastable ions has longer lifetimes than their time of transit through the beam line to the target. The metastable carbon ions with charge state 4+ allow some electron capture contributions similar to that of the carbon ions with charge state 5+ during the collision since they also have one K-shell vacancy. As a result, the metastable state condition contributes a small enhancement to the x-ray production cross sections as seen in Fig. 2 at 10 MeV. For 12-MeV incident ^{12}C ions, the appearance of metastable states is expected to be more prominent than that at 10 MeV. Unfortunately, we obtained no data on the cross section for charge state 3+ at 12 MeV because of the low carbon beam current at this energy. It can be seen from Fig. 2 for carbon ions with K vacancies ($q=5$ and 6) that the cross section increases from 35% to 200% as compared to the data for $q=4$. Since DI is essentially charge-state independent, the increase in cross sections for charge states 5+ and 6+ is attributed to the contributions of EC.

Figure 3 shows the measured K-shell x-ray production cross sections as a function of the ion beam energy for the Al target with thickness 0.14 μg/cm^2. The ECPSSR theory using single-hole fluorescence yields is shown as the solid curve. As can be seen in the figure, the ECPSSR theory gives a good fit to the data with discrepancies of 20% to 30% for DI+EC to L, M, ... shells for carbon ion with charge states 2+, 3+, and 4+ at energies 4–10 MeV (EC is included even though it is much smaller than DI for these charge states) while it overpredicts the data of the carbon ions with K vacancies ($q=5$ and 6) for DI+EC to K, L, M, ... shells by about 30% to 60 %. At 2 MeV, the ECPSSR theory underestimates the data by a factor of 2.6. This significant deviation appears at the lowest energy where the molecular-orbital ionization could become important [62–64].

Electron capture to the S ($S=K$, L, and M, ...) shell of an incident ion can only occur if the ion has a vacancy in that shell. For the K shell, the x-ray production cross section due to direct ionization plus electron capture for carbon ions with charge state q is given by

$$\sigma_{KX}=\sigma_{KX}^{\mathrm{DI}}+\sigma_{KX}^{\mathrm{EC}}. \tag{2}$$

If the direct ionization contributions are assumed to be approximately the same for carbon ions with different charge states, i.e., the effects of interactions between the projectile electrons and the target electrons are assumed to be small, the K-shell x-ray production cross section due to electron capture for double K vacancies in the carbon ion is then given by

$$\sigma_{KX}^{\mathrm{EC}(K\mathrm{shell})}=\sigma_{KX}^{\mathrm{EC}(K,L,M,\ldots\mathrm{shells})+\mathrm{DI}}-\sigma_{KX}^{\mathrm{EC}(L,M,\ldots\mathrm{shells})+\mathrm{DI}}, \tag{3}$$

which also implies the L-, M-, ... shell EC is basically the same for ions with and without K vacancies. The K-shell x-ray production cross section due to electron capture for one K vacancy is then given by

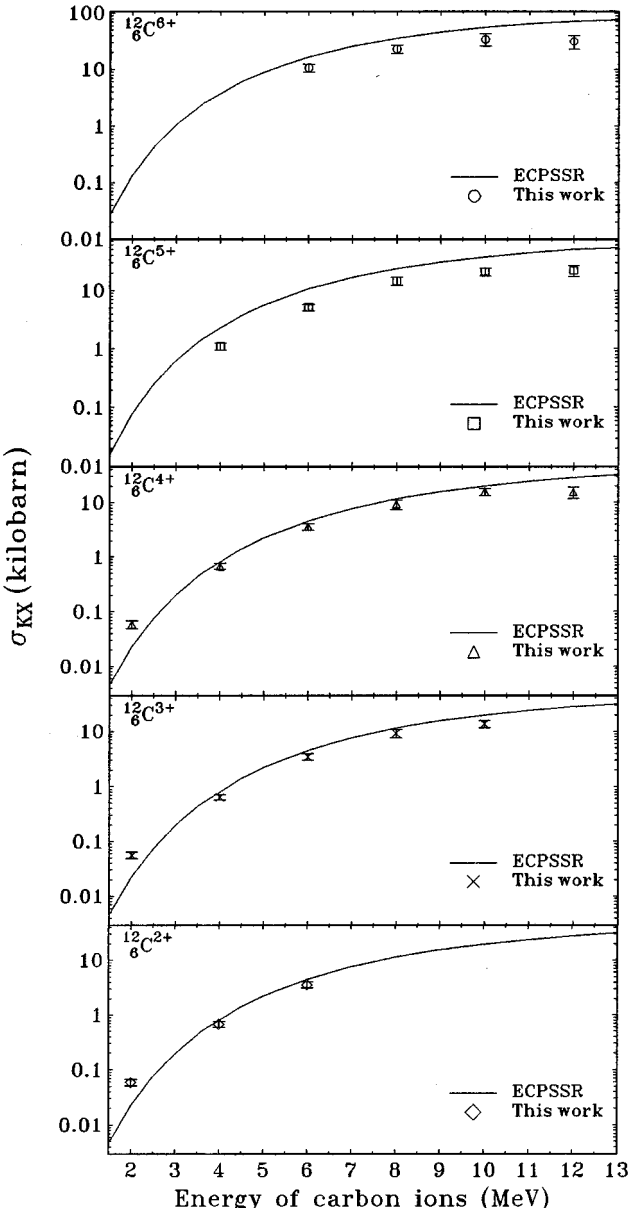

FIG. 3. K-shell x-ray production cross sections in $_{13}$Al for carbon ions with charge states 2+, 3+, 4+, 5+, and 6+. Curves are calculated from the ECPSSR theory [14–16].

$$\sigma_{KX}^{\mathrm{EC}(1/2K\mathrm{shell})} = \sigma_{KX}^{\mathrm{EC}(1/2K,L,M,\ldots\ \mathrm{shells})+\mathrm{DI}} - \sigma_{KX}^{\mathrm{EC}(L,M,\ldots\mathrm{shells})+\mathrm{DI}}, \quad (4)$$

where $\frac{1}{2}K$ and K represent a half vacant and completely vacant K shell for the incident carbon ions, respectively. In Eqs. (3) and (4) the DI is assumed to be the same, and independent of the number of electrons on the ion.

Table II tabulates all contributions of electron capture to the Al K-shell x-ray production cross sections. The ratios of the extracted $\sigma_{KX}^{\mathrm{EC}}(q)$ to the calculated $\sigma_{KX}^{\mathrm{EC-ECPSSR}}(q)$ are also listed. The EC cross sections $\sigma_{KX}^{\mathrm{EC}}(q)$ for $q=5$ and 6 were obtained, respectively, by a subtraction of $\sigma_{KX}(q)$ for $q=4$ or 3 from the x-ray production cross sections $\sigma_{KX}(q)$ for $q=5$ or 6. As seen in the third column of Table II, $\sigma_{KX}^{\mathrm{EC}}(q)$ values based on subtracting $\sigma_{KX}(q=4)$ or $\sigma_{KX}(q=3)$ and 3 show no significant differences at lower energies $E_1=4$, 6, and 8 MeV. However, the difference is noticeable at the higher energy $E_1=10$ MeV, arising from the metastable state formation as we discussed earlier for the results displayed in Fig. 2.

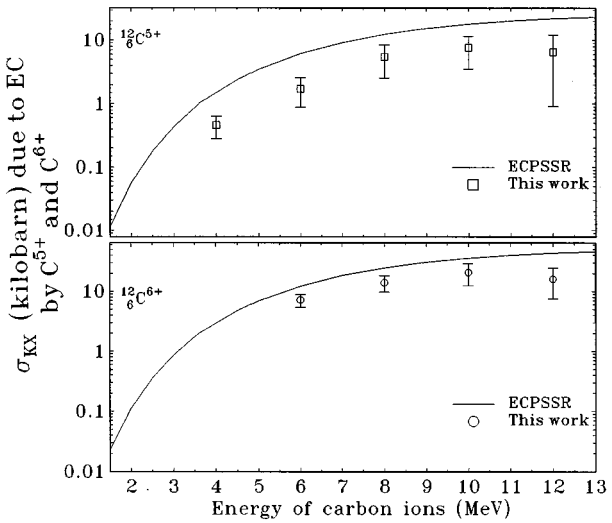

FIG. 4. K-shell x-ray production in $_{13}$Al due to electron capture to $\frac{1}{2}K$ and K shell of the carbon ion as a function of the energy of the hydrogenlike ($q=5$) and fully stripped ($q=6$) carbon ions. The curves represent the ECPSSR calculations for the electron capture [15,16].

Figure 4 shows the extracted x-ray production cross sections due to electron capture to $\frac{1}{2}K$ and K shell for carbon ions with charge states 5+ and 6+. The ECPSSR prediction is seen to overpredict the measurements by a factor of 2 to 4. Although the ECPSSR theory for EC [15,16] is an improvement over the OBKN approximation [11], a significant deviation from the measurement still exists.

IV. CONCLUSION

K-shell x-ray production cross sections of $_{13}$Al have been measured for carbon ions with various charge states as a function of target thicknesses (see Fig. 1). All of the measurements of charge-state dependencies of K-shell x-ray production were made for an ultrathin Al target (0.14 μg/cm^2) for 2–12 MeV $_6C^{q+}$ ($q=2$–6) ions. The Al K-shell x-ray production cross sections were found to be essentially independent of the projectile charge state with filled K shells (see Fig. 2 for $q=2$–4 at 2–8 MeV). When the carbon ion was energetic enough, the metastable phenomenon for $q=4$ gave a slightly higher cross section as compared to the data for $q=3$ (see Fig. 2 at 10 MeV). For carbon ions with K vacancies, the enhancement of the target x-ray production cross sections was observed because of electron capture to the K shell of the ion. In comparing the experimental K-shell x-ray production cross sections for both DI and EC (see Fig. 3), we found that the ECPSSR theory overpredicts the data by 20% to 45% for $q=2$–4 and factors of 1.5 to 2.3 for $q=5$ and 6 while it underestimates all the data at 2 MeV about 60%. The underprediction of the measurements at the lowest energy might be due to the opening of an efficient channel for ionization via molecular-orbital promotion which has not been included in the ECPSSR theory. The measured electron cap-

ture cross sections have been determined by subtracting the $q=3$ or 4 data from the $q=5$ and 6 data for vanishingly thin targets (0.14 $\mu g/cm^2$) and compared with the ECPSSR theory (see Fig. 4). The ECPSSR theory is seen to exceed the data by a factor of 2 for the C^{6+} and for the energy range 6–12 MeV. The C^{5+} data are on the average a factor of 3 below the present calculations for electron capture.

ACKNOWLEDGMENTS

This work is partial supported by National Science Council of the Republic of China under Grant No. NSC85-2112-M-001-012-Y, National Science Foundation of the United States of America under Grant No. NSF-INT-9320368, the Robert A. Welch Foundation, and the U.S. Office of Naval Research.

[1] J. R. Macdonald, L. Winters, M. D. Brown, T. Chiao, and L. D. Ellsworth, Phys. Rev. Lett. **29**, 1291 (1972).
[2] F. D. McDaniel, J. L. Duggan, G. Lapicki, and P. D. Miller, Nucl. Instrum. Methods Phys. Res. Sect. B **42**, 485 (1989).
[3] E. Merzbacher and H. Lewis, in *Encylopedia of Physics*, edited by S. Flügge, Handbüch der Physik Vol. 34 (Springer, Berlin, 1958), p. 166.
[4] A. M. Halpern and J. Law, Phys. Rev. Lett. **31**, 4 (1973).
[5] U. Fano and W. Lichten, Phys. Rev. Lett. **14**, 627 (1965); W. Lichten, Phys. Rev. **164**, 131 (1967).
[6] D. H. Madison and E. Merzbacher, in *Atomic Inner-Shell Processes*, edited by B. Crasemann (Academic, New York, 1975), Vol. 1, pp. 1–72.
[7] R. Rice, G. Basbas, and F. D. McDaniel, At. Data Nucl. Data Tables **20**, 503 (1977).
[8] J. Bang and J. M. Hansteen, K. Dan. Vidensk. Selsk, Mat.-Fys. Medd. **31**, No. 13, 1 (1959); J. M. Hansteen and O. P. Mosebekk, Z. Phys. **234**, 281 (1970).
[9] J. D. Garcia, Phys. Rev. A **1**, 280 (1970); J. S. Hansen, *ibid.* **8**, 822 (1973).
[10] R. K. Gardner, T. J. Gray, P. Richard, C. Schmiedekamp, K. A. Jamison, and J. M. Hall, Phys. Rev. A **19**, 1896 (1979).
[11] V. S. Nikolaev, Zh. Éksp. Teor. Fiz. **51**, 1263 (1966) [Sov. Phys. JETP **24**, 847 (1967)].
[12] J. R. Oppenheimer, Phys. Rev. **31**, 349 (1928).
[13] H. C. Brinkman and H. A. Kramers, Proc. Acad. Sci. (Amsterdam) **33**, 973 (1930).
[14] W. Brandt and G. Lapicki, Phys. Rev. A **23**, 1717 (1981).
[15] G. Lapicki and W. Losonsky, Phys. Rev. A **15**, 896 (1977).
[16] G. Lapicki and F. D. McDaniel, Phys. Rev. A **22**, 1896 (1980); **23**, 975(E) (1981).
[17] H. Paul and J. Muhr, Phys. Rep. **135**, 47 (1986).
[18] G. Lapicki, J. Phys. Chem. Ref. Data **18**, 111 (1989).
[19] J. R. Mowat, I. A. Sellin, P. M. Griffin, D. J. Pegg, and R. S. Peterson, Phys. Rev. A **9**, 644 (1974).
[20] S. J.Czuchlewski, J. R. Macdonald, and L. D. Ellsworth, Phys. Rev. A **11**, 1108 (1975).
[21] J. R. Macdonald, L. M. Winters, M. D. Brown, L. D. Ellsworth, T. Chiao, and E. W. Pettus, Phys. Rev. Lett. **30**, 251 (1973).
[22] J. R. Mowat, D. J. Pegg, R. S. Peterson, P. M. Griffin, and I. A. Sellin, Phys. Rev. Lett. **29**, 1577 (1972).
[23] S. Datz, B. R. Appleton, J. R. Mowat, R. Laubert, R. S. Peterson, R. S. Thoe, and I. A. Sellin, Phys. Rev. Lett. **33**, 733 (1973).
[24] W. Brandt, R. Laubert, M. Maurino, and A. Schwarzschild, Phys. Rev. Lett. **30**, 358 (1973).
[25] J. R. Macdonald, C. L. Cocke, and W. W. Edison, Phys. Rev. Lett. **32**, 648 (1974).
[26] F. Hopkins, R. L. Kauffman, C. W. Woods, and P. Richard, Phys. Rev. A **9**, 2413 (1974).
[27] J. R. Macdonald, M. D. Brown, S. J. Czuchlewski, L. M. Winters, R. Laubert, I. A. Sellin, and J. R. Mowat, Phys. Rev. A **14**, 1997 (1976).
[28] T. J. Gray, P. Richard, K. A. Jamison, J. M. Hall, and R. K. Gardner, Phys. Rev. A **14**, 1333 (1976).
[29] J. A. Guffey, L. D. Ellsworth, and J. R. Macdonald, Phys. Rev. A **15**, 1863 (1977).
[30] R. K. Gardner, T. J. Gray, P. Richard, C. Schmiedekamp, K. A. Jamison, and J. M. Hall, Phys. Rev. A **15**, 2202 (1977).
[31] U. Schiebel, T. J. Gray, R. K. Gardner, and P. Richard, J. Phys. B **10**, 2189 (1977).
[32] H. Tawara, P. Richard, T. J. Gray, J. Newcomb, K. A. Jamison, C. Schmiedekamp, and J. M. Hall, Phys. Rev. A **18**, 1373 (1978).
[33] T. J. Gray, P. Richard, G. Gealy, and J. Newcomb, Phys. Rev. A **19**, 1424 (1979).
[34] A. Schmiedekamp, T. J. Gray, B. L. Doyle, and U. Schiebel, Phys. Rev. A **19**, 2167 (1979).
[35] F. D. McDaniel, J. L. Duggan, G. Basbas, P. D. Miller, and G. Lapicki, Phys. Rev. A **16**, 1375 (1977).
[36] F. D. McDaniel, A. Toten, R. S. Peterson, J. L. Duggan, S. R. Wilson, J. D. Gressett, P. D. Miller, and G. Lapicki, Phys. Rev. A **19**, 1517 (1979).
[37] R. Mehta, J. L. Duggan, F. D. McDaniel, M. C. Andrews, G. Lapicki, P. D. Miller, L. A. Rayburn, and A. R. Zander, Phys. Rev. A **28**, 2722 (1983).
[38] M. C. Andrews, F. D. McDaniel, J. L. Duggan, P. D. Miller, P. L. Pepmiller, H. F. Krause, T. M. Rosseel, L. A. Rayburn, R. Mehta, and G. Lapicki, Nucl. Instrum. Methods Phys. Res. Sect. B **10/11**, 186 (1985).
[39] M. C. Andrews, F. D. McDaniel, J. L. Duggan, P. D. Miller, P. L. Pepmiller, H. F. Krause, T. M. Rosseel, L. A. Rayburn, R. Mehta, and G. Lapicki, Phys. Rev. A **36**, 3699 (1987).
[40] H. L. Sun, J. L. Duggan, F. D. McDaniel, and G. Lapicki, Nucl. Instrum. Methods Phys. Res. Sect. B **99**, 192 (1995).
[41] Y. C. Yu, H. L. Sun, J. L. Duggan, F. D. McDaniel, J. Y. Jin, and G. Lapicki, Phys. Rev. A **52**, 3836 (1995).
[42] Yissum Research Development Company of the Hebrew University of Jerusalem, 46 Jabotinsky St., P.O. Box 4279, Jerusalem, 91042 Israel.
[43] D. L. Weathers, J. L. Duggan, M. R. McNeir, Y. C. Yu, F. D. McDaniel, C. A. Quarles, H. Lehtihet, and D. Kahler, Nucl. Instrum. Methods Phys. Res. Sect. B **56/57**, 964 (1991).
[44] D. L. Weathers, J. L. Duggan, R. B. Escue, and F. D. McDaniel, Nucl. Instrum. Methods Phys. Res. Sect. A **303**, 69 (1991).

[45] F. D. McDaniel, D. K. Marble, J. L. Duggan, M. R. McNeir, Y. C. Yu, Z. Y. Zhao, D. L. Weathers, R. M. Wheeler, R. P. Chaturvedi, and G. Lapicki, Nucl. Instrum. Methods Phys. Res. Sect. B **53**, 531 (1991).
[46] J. F. Ziegler, TRIM program, the upgraded 1900 version.
[47] R. Laubert, H. Haselton, J. R. Mowat, R. S. Peterson, and I. A. Sellin, Phys. Rev. A **11**, 135 (1975).
[48] W. J. Veigele, At. Data **5**, 51 (1973).
[49] M. O. Krause, J. Phys. Chem. Ref. Data **8**, 307 (1979).
[50] O. Benka, Nucl. Instrum. Methods Phys. Res. Sect. B **4**, 279 (1984).
[51] P. Richard, I. L. Morgan, T. Furuta, and D. Burch, Phys. Rev. Lett. **23**, 1009 (1969).
[52] P. Richard, T. I. Bonner, T. Furuta, I. L. Morgan, and J. R. Rhodes, Phys. Rev. A **1**, 1044 (1970).
[53] D. Burch and P. Richard, Phys. Rev. Lett. **25**, 983 (1970).
[54] D. K. Olsen, C. F. Moore, and P. Richard, Phys. Rev. A **7**, 1244 (1973).
[55] L. Winters, J. R. Macdonald, M. D. Brown, T. Chiao, L. D. Ellsworth, and E. W. Pettus, Phys. Rev. A **8**, 1835 (1973).
[56] D. Burch, N. Stolterfoht, D. Schneider, H. Wieman, and J. S. Risley, Phys. Rev. Lett. **32**, 1151 (1974).
[57] T. W. Tunnell, C. Can, and C. P. Bhalla, IEEE Trans. Nucl. Sci. **NS-26**, 1124 (1979).
[58] J. A. Tanis, S. M. Shafroth, W. W. Jacobs, T. McAbee, and G. Lapicki, Phys. Rev. **31**, 75 (1985).
[59] A. R. Knudsen, D. J. Nagel, P. G. Burkhalter, and K. L. Dunning, Phys. Rev. Lett. **26**, 1149 (1971).
[60] I. Sellin, Adv. At. Mol. Phys. **12**, 215 (1977).
[61] C. D. Lin, W. R. Johnson, and A. Dalgarno, Phys. Rev. A **15**, 154 (1977).
[62] M. Vigilante, P. Cuzzocrea, N. De Cesare, F. Muroolo, E. Perillo, and G. Spadaccini, Nucl. Instrum. Methods Phys. Res. Sect. B **51**, 232 (1990).
[63] M. Geretschläger, Ž. Šmit, and O. Benka, Phys. Rev. A **41**, 123 (1990).
[64] M. Geretschläger, Ž. Šmit, and E. Steinbauer, Phys. Rev. A **45**, 2842 (1992).